Inhibition of cellular senescence by developmentally regulated FGF receptors in mesenchymal stem cells

*Daniel L. Coutu,[1,2] *Moïra François,[1,2] and Jacques Galipeau[1-4]

[1]Division of Experimental Medicine, McGill University, Montreal, QC; [2]Sir Mortimer B. Davis Jewish General Hospital and Lady Davis Institute for Medical Research, Montreal, QC; and Departments of [3]Hematology and Medical Oncology and [4]Pediatrics, Emory University, Winship Cancer Institute, Atlanta, GA

Bone-derived mesenchymal stem cells (MSCs) are important cells for use in cell therapy, tissue engineering, and regenerative medicine, but also to study bone development, homeostasis, and repair. However, little is known about their developmental ontology and in vivo identity. Because fibroblast growth factors (FGFs) play key roles in bone development and their receptors are developmentally regulated in bones, we hypothesized that MSCs should express FGF receptors (FGFRs), reflecting their developmental origin and potential. We show here that FGFR1/2 are expressed by rare mesenchymal progenitors in putative MSC niches in vivo, including the perichondrium, periosteum, and trabecular marrow. FGFR1$^+$ cells often appeared as pericytes. These cells display a characteristic MSC phenotype in vitro when expanded with FGF-2, which appears to maintain MSC stemness by inhibiting cellular senescence through a PI3K/AKT-MDM2 pathway and by promoting proliferation. FGFRs may therefore be involved in MSC self-renewal. In summary, FGFR1/2 are developmentally regulated markers of MSCs in vivo and in vitro and are important in maintaining MSC stemness. (*Blood*. 2011; 117(25):6801-6812)

Introduction

Mesenchymal stem cells (MSCs) are stem/progenitor cells for bone, cartilage, and hematopoietic-supporting marrow stroma (including bone-lining cells, fibroblasts, reticulocytes, adipocytes, and pericytes). However, the fundamental study of these intriguing cells is currently limited by uncertainties regarding their ontology, in vivo identity, and developmental potential. This is complicated by the lack of molecular markers and standard isolation procedures and by difficulties in studying MSCs in mouse models.[1-3] Recently, 2 different studies provided evidence that undifferentiated mesenchymal cells are present in murine embryonic perichondrium during endochondral bone formation.[4-7] These cells were shown to adopt a pericyte identity while migrating from the perichondrium to colonize both the bone collar (cortical bone) and the primary spongiosa (trabecular bone). Moreover, these cells were shown to participate in fracture repair in postnatal bones. These observations are significant because they are the first to unambiguously demonstrate that perichondrium-derived cells participate in both cortical bone and trabecular bone formation and give rise to osteostromal progenitors that have a marrow perivascular niche, which was previously proposed for human MSCs.[8,9] Moreover, these studies reconcile contradictory reports demonstrating the presence of MSCs in cortical bone, trabecular bone, periosteum, and the marrow/periosteal perivascular space.[10-16]

Endochondral bone formation, homeostasis, and repair are highly orchestrated processes involving cellular proliferation, migration, differentiation, and apoptosis, as well as cross-talk between the growth plate, perichondrium/periosteum, cortical and trabecular bone, marrow stroma, and invading vasculature and hematopoietic cells.[17-19] In addition to mechanical, nervous, and endocrine stimulation, these events are largely mediated by soluble factors such as PDGF, TGF-β, BMPs, Wnts, parathyroid hormone–related protein (PTHrP), Indian hedgehog (Ihh), and FGFs, and their associated receptors. The FGF family comprises 22 ligands displaying high levels of homology, redundancy, and promiscuity. There are 4 known FGF receptors (FGFRs) expressed as multiple splice variants, and 3 of them are involved in bone formation: FGFR1, FGFR2, and FGFR3. FGFs/FGFRs are expressed in a tissue-specific manner, are developmentally regulated, and are crucial for bone formation, maintenance, and repair.[20] However, the large number of ligands and receptor isoforms, as well as their redundancy and promiscuity, makes the study of their roles in endochondral bone formation a particular challenge. The mitogenic effect of FGF-2 on MSCs in vitro has long been observed, and studies have also shown that FGF-2 promotes undifferentiated proliferation of MSCs in vitro.[21-25] However, given the importance of FGFs/FGFRs in bone, it is surprising that this system has not yet been described in more detail in MSCs.

In the present study, we hypothesized that MSCs should express FGFRs, reflecting their developmental origin/potential, and that these markers could be used to identify MSCs in vivo and in vitro (similar to how the SLAM markers are now used for hematopoietic stem cells).[26] We provide evidence that FGFR1/2 are expressed by MSCs in vivo and in vitro and are developmentally regulated during their differentiation. Furthermore, we found that FGFR1/2 signaling through PI3K/AKT-MDM2 promotes the proliferation of MSCs mainly by inhibiting cellular senescence while maintaining MSC properties. Therefore, FGFR1/2 may be mediators of self-renewal (defined as maintenance of stemness during proliferation) in murine MSCs and can be used as markers to identify MSCs in situ and by flow cytometry.

Submitted December 3, 2010; accepted April 18, 2011. Prepublished online as *Blood* First Edition paper, April 28, 2011; DOI 10.1182/blood-2010-12-321539.

*D.L.C. and M.F. contributed equally to this study.

The online version of this article contains a data supplement.

The publication costs of this article were defrayed in part by page charge payment. Therefore, and solely to indicate this fact, this article is hereby marked "advertisement" in accordance with 18 USC section 1734.

Methods

MSC isolation

All experimental procedures involving murine and human material were approved by the Lady Davis Institute Ethics Review Board. Human MSCs were obtained from marrow biopsies of volunteers undergoing hip replacement, isolated by Ficoll gradient and plastic adherence, and expanded in α-MEM with 20% FBS (Wisent Bioproducts). Murine MSCs from female C57Bl/6 mice (Harlan) were obtained (unless otherwise specified) from whole bones digested in PBS containing 2% FBS, 2.5 mg/mL of collagenase I (Sigma-Aldrich), 0.7 mg/mL of collagenase II (Worthington), and 1 U/mL of dispase (GIBCO) for 1 hour at 37°C, then crushed using a sterile pestle. MSCs were grown in DMEM (HyClone) with 10% FBS. FGF-2, epidermal growth factor (EGF), PDGF (Feldan Bio), and TGF-β1 (Austral Biologicals) were used at a 5 ng/mL concentration unless otherwise specified. Sodium heparin (5 U/mL; Sigma-Aldrich) was added as a cofactor for FGF-2. MSCs were passaged at 5000cells/cm^2 weekly or at confluence, whichever came first.

CFU-F assays

For a description of the CFU-F assays, see supplemental Methods (available on the *Blood* Web site; see the Supplemental Materials link at the top of the online article).

Senescence-associated β-galactosidase assay

MSCs were isolated and treated as indicated in 6-well plates, then fixed with 4% paraformaldehyde and stained with 5-bromo-4-chloro-3-indolyl β-D-galactopyranoside (X-Gal) overnight. The staining solution consisted of: PBS, citric acid/phosphate buffer (final concentrations: 20mM citric acid, 40mM sodium phosphate, pH 5.5), 5mM potassium-ferricyanide, 5mM potassium-ferrocyanide, 150mM NaCl, 2mM $MgCl_2$, and 1 mg/mL X-Gal.

Western blot

Passage-0 MSCs were enriched with the EasySep Mouse Mesenchymal Stem/Progenitor Cell Enrichment Kit (StemCell Technologies) and treated with the indicated growth factors and/or the PI3K inhibitor LY294002 (Cell Signaling Technology). After SDS-PAGE separation and transfer to PVDF membranes, blots were probed using the specified antibodies. Densitometry was done using ImageJ v1.43m (National Institutes of Health).

Antibodies and fluorescent labels

A complete list of the antibodies and labels used can be found in supplemental Methods.

Flow cytometry

Labeling was performed using standard procedures and acquisition was on a FACSCalibur flow cytometer (BD Biosciences).

MHC class I–mediated antigen presentation

MSCs were stimulated with rmIFN-γ and pulsed with OVA (1 mg/mL; Sigma-Aldrich) for 18 hours. Cells were harvested, washed, and serially diluted in flat-bottomed, 96-well plates. K^b-restricted OVA-specific (257-264 SIINFEKL epitope) $CD8^+$ T cells from C57BL/6-Tg(TcraTcrb)1100Mjb (OT-I) mice (The Jackson Laboratory) spleens were enriched using the EasySep Mouse $CD8^+$ T-Cell Enrichment Kit (StemCell Technologies), and 10^5 cells were added to the wells (> 98% purity by FACS; not shown). IL-2 produced by activated T cells was quantified at 48 hours by ELISA (eBioscience).

MLR

MSCs were seeded as indicated in a round-bottomed, 96-well plate and splenocytes from Balb/c and C57Bl/6 mice were added at the indicated ratios (MSC:splenocytes). IL-2 produced by activated T cells was quantified at 72 hours using ELISA.

In vitro differentiation

For a description of the in vitro differentiation procedures, see supplemental Methods.

In vivo differentiation

MSCs (10^6) were incubated with 40 mg of hydroxyapatite/tricalcium phosphate (HA/TCP) ceramic particles (250-μm diameter, HA:TCP ratio 60:40; Plasma Biotal) at 37°C for 2 hours. The suspension was centrifuged, mixed in a collagen I gel, and implanted subcutaneously for 8 weeks.

Histology and immunofluorescence

Implants were harvested and fixed with formalin, decalcified in 5% EDTA, and processed for regular histology. Undecalcified tissues were embedded in methylmethacrylate for von Kossa and Toluidine Blue staining. For whole-mount immunofluorescence, bones from embryonic or postnatal mice were fixed in ice-cold methanol and washed in methanol/acetone (3:1). Coverslips were fixed with 4% formalin and permeabilized with 0.2% Triton X-100 (Sigma-Aldrich). Normal donkey serum (10%) was used for blocking.

Light and confocal microscopy

Light microscopy was done on a Leica DM-LB2 microscope equipped with a Leica DFC480 camera and acquired using the Leica Application Suite. Confocal microscopy was done on a WaveFX/Leica spinning-disk confocal microscope. Image acquisition, 3D reconstruction, surface rendering, and colocalization were done using Volocity 4 and Imaris 5 software. Z-stacks covering the entire sample were acquired at 0.3-0.5 μm and 1-3 μm for coverslips and bone specimens, respectively. All images are 3D reconstructions of the entire dataset without deconvolution. Surface rendering was only used for the images shown in Figure 2E. Quantification of nuclear p-MDM2 was performed by counting the total voxels positive for p-MDM2 and 4′,6-diamidino-2-phenylindole, dihydrochloride (DAPI). For Ki67 quantification, the number of $Ki67^+$ nuclei was counted in 5 randomly chosen low-power fields or until 50 cells were counted.

Real-time quantitative PCR

RNA was extracted from MSCs using the RNeasy kit with DNAse (QIAGEN). RNA (2 μg) was reverse transcribed with MuLV reverse transcriptase (Applied Biosystems) using random hexamers and RNAse inhibitor. Real-time quantitative PCR (RT-qPCR) assays were performed in duplicate on an ABI 7500 Fast Real-Time PCR system thermal cycler using the SYBR Green Fast Master Mix (Applied Biosystems). The primers used are described in supplemental Tables 1 and 2. Data were quantified by comparing with 18S RNA. Specificity was tested by melting-curve analysis. The absence of genomic DNA was demonstrated by PCR performed with total RNA for each primer set.

Irradiation of cells and animals

Animals were sublethally irradiated at 9 Gy and killed 10 days later. MSCs seeded on coverslips at passage 3 (50% confluence) were irradiated at 10 Gy and then placed in fresh medium and processed 7 days after irradiation

Statistical analyses

Histograms are presented as means ± SEM. Student *t* tests and ANOVA were done using GraphPad Prism 5. Immunostainings were performed at

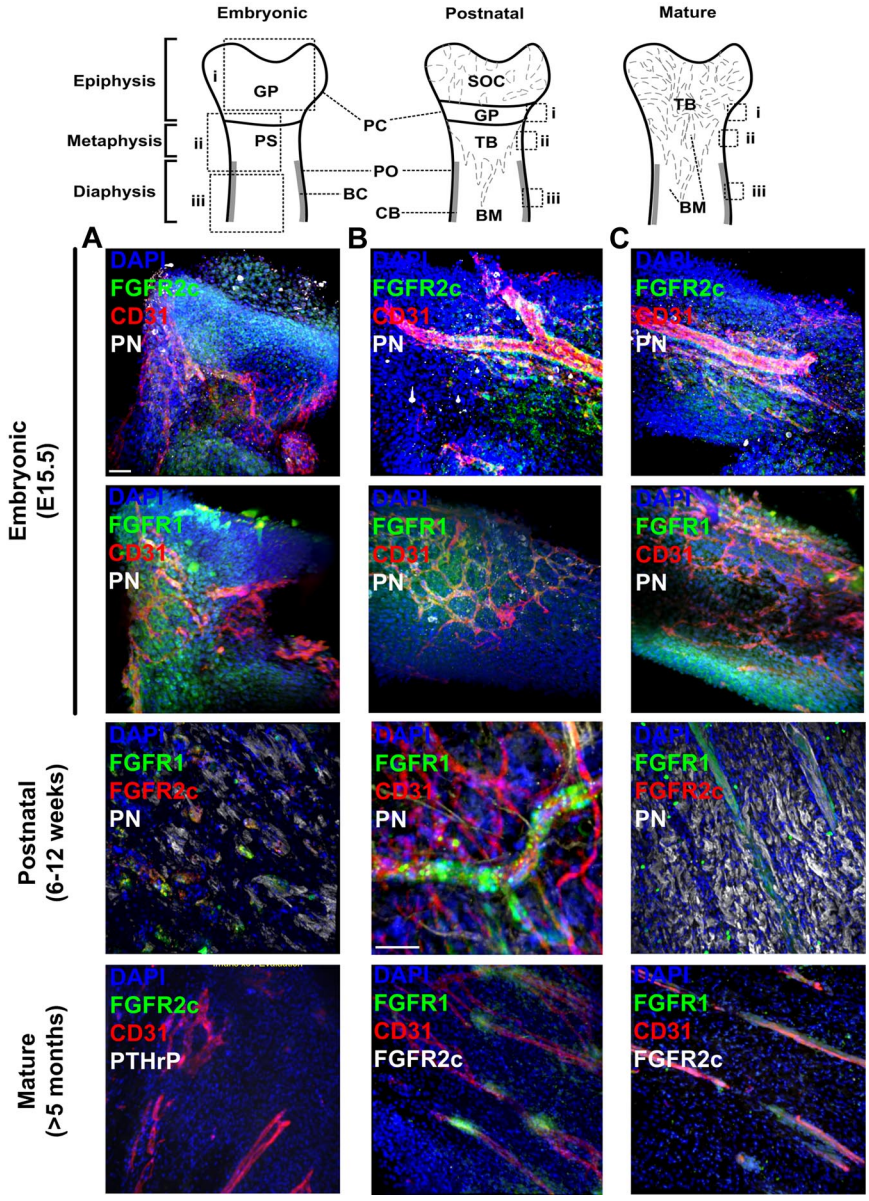

Figure 1. Localization of FGFR1/2$^+$ cells in embryonic, postnatal, and mature bones. Shown is whole-mount immunofluorescence staining of murine bones analyzed by confocal microscopy with 3D reconstruction. For each sample, images of the epiphysis (A), metaphysis (B), and diaphysis (C) were acquired. For embryonic bones, E15.5 distal femurs are shown. For postnatal bones, perichondrium (PC) covering the anterior iliac ala and fossa and periosteum (PO) covering the iliac body are shown. CD31 was used to identify blood vessels, PN was used to visualized periosteum and preosteoblastic cells, PTHrP was used to identify early mesenchymal progenitors, and DAPI was used to stain cell nuclei. Z-stacks 100-300 μm in depth were acquired at 2-μm intervals for all channels to scan the irregular bone surfaces. Three-dimensional reconstruction was done using Imaris without deconvolution. GP indicates growth plate; PS, primary spongiosa; BC, bone collar; CB, cortical bone; SOC, secondary ossification center; and TB, trabecular bone. Scale bars indicate 50 μm.

least in triplicate. For other experiments, the numbers of replicates, animals, donors, or cells are indicated in the text.

Results

Developmental regulation of FGFR expression in bone

FGFR isoform expression in bone has been mostly studied during embryonic development, which clearly indicated that the receptors are developmentally regulated in skeletal tissues.[20] However, the irregular and asymmetric shape of bones makes it difficult to analyze FGFR expression at the single-cell level using multiple-lineage markers with traditional histology techniques (especially in the periosteum and perichondrium). To test our hypothesis that FGFRs can be used as markers of MSCs in vivo, we initially sought to localize and identify FGFR$^+$ cells in embryonic and postnatal bones. To this end, we used 4-color whole-mount immunofluorescence combined with low-power confocal microscopy, which allowed scanning and 3D reconstruction of irregular bone surfaces.

In embryonic day 15.5 (E15.5) mouse femurs (near the onset of bone collar formation), we found broad distribution of both FGFR1 and FGFR2 in the epiphyseal perichondrium covering growth plate cartilage and in the periosteum covering the metaphysis and diaphysis (Figure 1 top panels). In the highly vascular periosteum, FGFR2$^+$ cells are mainly perivascular, whereas FGFR1 shows a slightly broader expression pattern. The absence of the mesenchymal and preosteoblast marker periostin[27] (PN) in E15.5 periosteum suggested that bone collar formation was still at an early stage. In postnatal immature bones (before growth plate closure), FGFR2c was only detected in perichondrial cells that appeared as small mesenchymal condensations surrounded by a few PN$^+$ preosteoblasts (Figure 1 middle panels). These cells coexpressed FGFR1. In postnatal periosteum, FGFR1 could be detected in rare perivascular cells in both the metaphysis and diaphysis, whereas only rare FGFR2$^+$ pericytes could be detected in the metaphysis (not shown). We next analyzed FGFR expression in mature bones (after growth plate mineralization) and found no detectable FGFR2c expression in the now richly vascularized epiphyseal periosteum

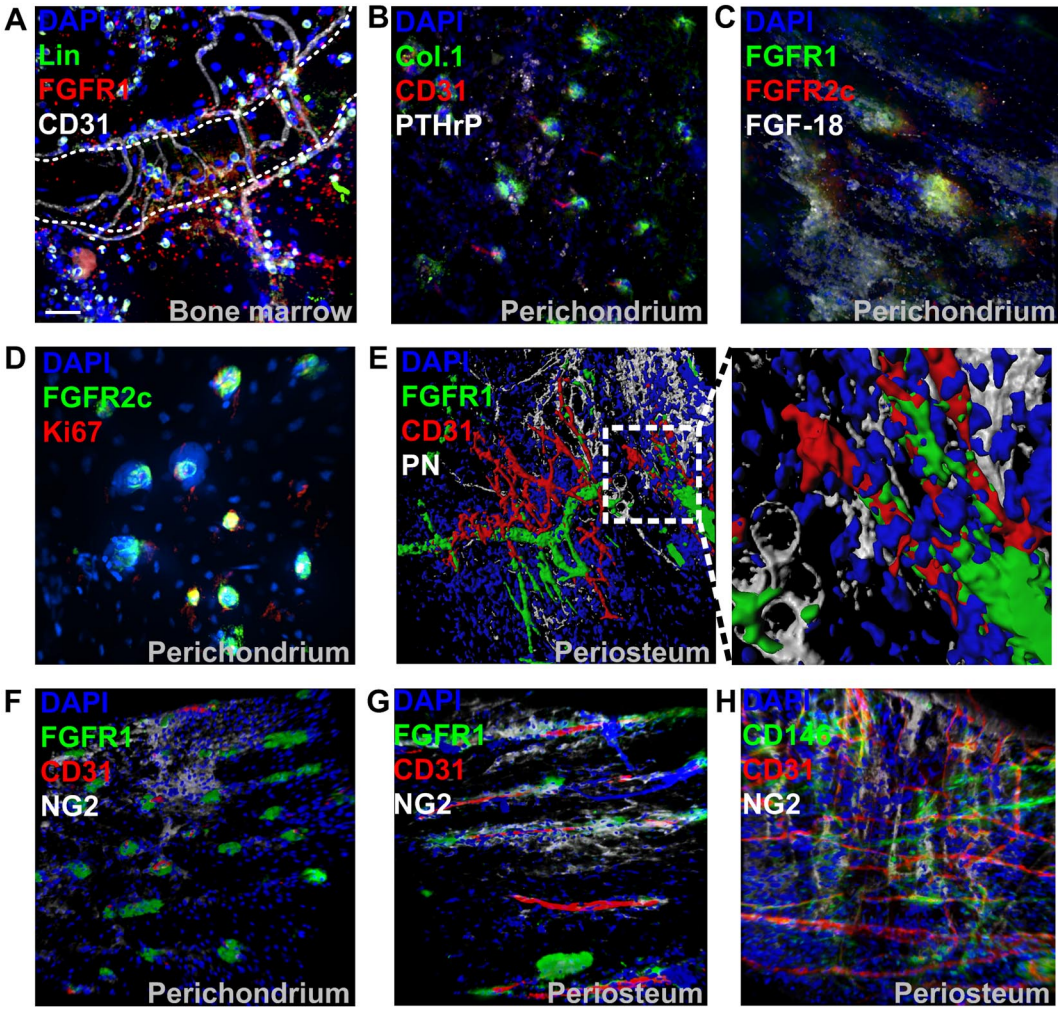

Figure 2. Characterization of FGFR1/2$^+$ skeletal cells in vivo. (A) Immunofluorescence of trabecular BM tissue section from anterior iliac visualized with confocal microscopy. A 3D reconstruction of a Z-stack of the whole 10-μm section taken at 0.3-μm intervals is shown. Hematopoietic lineage markers (Lin) and CD31 were used to exclude hematopoietic cells and endothelial cells, respectively. The dotted line shows a trabecular bone surface. (B) Whole-mount immunofluorescence staining of perichondrium (acquired as in Figure 1). Collagen 1 (Col.1) and PTHrP showed a similar expression pattern to FGFR1/2$^+$ cells in the perichondrium and were sometimes irrigated by CD31$^+$ microvasculature. (C) Cells surrounded by perichondrium-specific, FGF-18–expressing cells. The proliferation marker Ki67 was only detected in perichondrial cells and colocalized with FGFR1/2$^+$ cells (D). (E) Three D reconstruction and surface rendering demonstrating that most periosteal FGFR1$^+$ cells were pericytes wrapped around CD31$^+$ blood vessels. In the mostly avascular perichondrium, the pericyte marker NG2 did not colocalize with FGFR1$^+$ cells, but appeared to be expressed by chondrocytic progenitors (F). In vascularized periosteum, FGFR1$^+$/NG2$^+$ pericytes could be observed; however, not all FGFR1$^+$ cells coexpressed NG2, which was also detected in nonpericytic cells (G). Expression of the pericytic MSC marker CD146 in periosteum also showed only limited colocalization with NG2 (H).

(previously perichondrium). However, FGFR1 persisted in a subpopulation of periosteal pericytes (Figure 1 bottom panels).

Expression of FGFRs in putative MSCs in vivo

FGFR1 could also be detected in the marrow cavity of postnatal bones (Figure 2A). Hematopoietic lineage marker–negative (Lin$^-$)/CD31$^-$/FGFR1$^+$ cells were typically observed near both microvasculature (CD31$^+$) and trabecular surfaces. However, because of the high expression of FGFRs in hematopoietic tissue and the high level of autofluorescence in marrow, these cells were generally difficult to localize. To further characterize FGFR1/2$^+$ cells in vivo, we stained postnatal perichondrial tissue with antibodies against collagen 1 and PTHrP, 2 markers of putative osteostromal progenitors in the perichondrium.[6] We found that their distribution correlated well with that of FGFR1/2$^+$ cells in the perichondrium (Figure 2B). Interestingly, the loss of FGFR2 expression in mature bones was also correlated with the loss of PTHrP expression (Figure 1 bottom left panel). Perichondrial FGFR1/2$^+$ cells were also found to be surrounded by FGF-18–expressing cells (Figure 2C), whereas FGF-2 and FGF-8 were undetectable (not shown). However, FGF-18 activates FGFR1/2 only weakly, and it remains to be determined if this ligand has a direct effect on FGFR1/2$^+$ cells. The proliferation marker Ki67 also stained almost exclusively FGFR1/2$^+$ cells in the perichondrium (Figure 2D and supplemental Figure 1A) and was undetectable in the periosteum, where most cells appeared quiescent (not shown).

Surface rendering of confocal data confirmed that FGFR1 was only expressed by perivascular cells and not by CD31$^+$ endothelial cells or PN$^+$ preosteoblasts (Figure 2E). To confirm that FGFR1$^+$ cells were indeed pericytes, we analyzed their expression of the pericyte marker NG2 (Figure 2F-G), and observed that FGFR1/2$^+$ cells in the avascular perichondrium did not express NG2, which was instead expressed by chondrogenic progenitors, as described previously.[28] Conversely, some periosteal FGFR1$^+$ cells did coexpress NG2, but the expression patterns of those 2 markers were not completely overlapping. Similarly, CD146, another marker of pericytic MSCs, did not show extensive colocalization with NG2 (Figure 2H). Unfortunately, the only antibody against murine

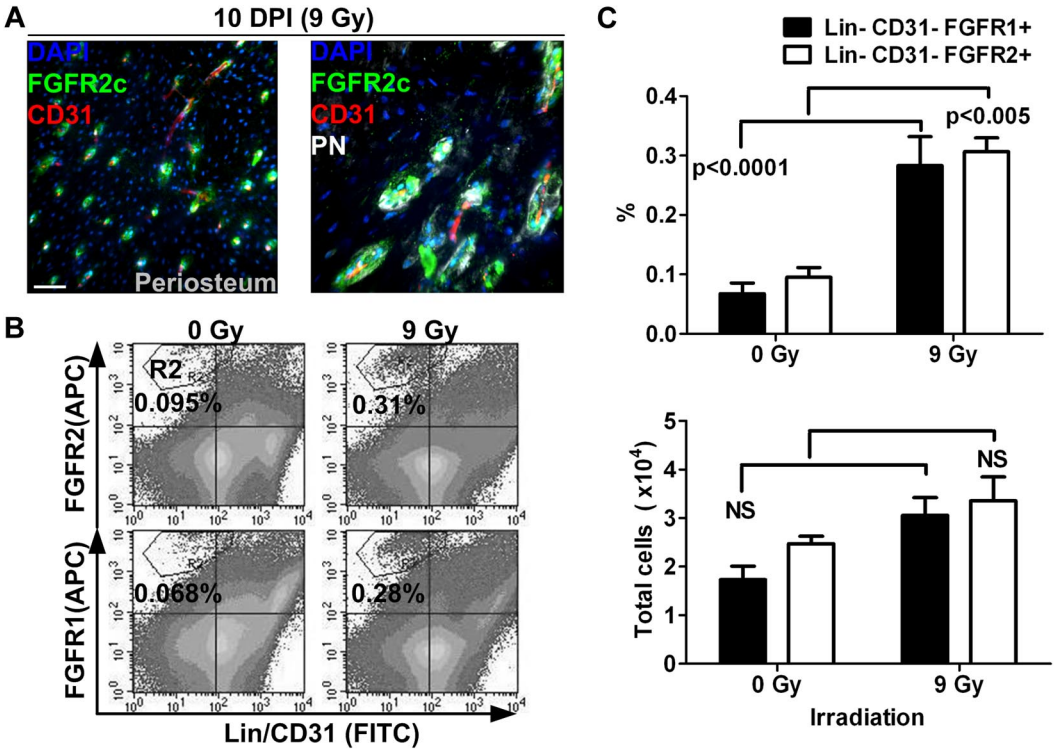

Figure 3. Distribution and quantification of FGFR1/2$^+$ mesenchymal cells after sublethal TBI. (A) Ten days after irradiation (10 DPI) at 9 Gy, the periosteum showed evidence of intense remodeling and FGFR2$^+$ cells were observed in vascularized PN$^+$ canals on the cortical bone surface (see also supplemental Figure 1B). Scale bar indicates 50 μm. (B) Flow cytometric quantification of FGFR1$^+$ and FGFR2$^+$ mesenchymal cells in whole bones 10 days after sublethal irradiation. (C) Cells in the R2 region (Lin$^-$/CD45$^-$/FGFR1 or 2$^+$) were compared with total cell numbers obtained from 5 nonirradiated control mice and 10 irradiated test mice. The frequency (%) of FGFR1/2$^+$ cells was increased after irradiation, but their absolute number was relatively stable, suggesting that these cells are radio-resistant. APC indicates allophycocyanin.

CD146 we found useful for immunofluorescence was not compatible with our FGFR1 antibody. Nevertheless, if FGFR1/2$^+$ mesenchymal cells are indeed MSCs, these data suggest that not all MSCs are pericytes (eg, in the perichondrium), that not all pericytes are MSCs, and that not all pericytes are the same within a given tissue.

Analysis of FGFR expression during tissue repair

To better understand the role of FGFR1/2$^+$ cells in bone, we next sought to determine whether they are involved in tissue remodeling after injury. To do this, we analyzed the distribution and frequency of FGFR1/2$^+$ cells in bones 10 days after sublethal irradiation (9 Gy). It is well known that total body irradiation (TBI) induces important changes in the cellular content of the BM, including disruption of marrow sinusoids, disappearance of most hematopoietic cells, and differentiation of stromal cells into adipocytes. In the present study, we observed that irradiation also induces important changes in the periosteum (Figure 3A). In the diaphyseal periosteum, we observed an almost complete disappearance of the PN$^+$ preosteoblastic cell layer after TBI, whereas FGFR2$^+$ cells could be observed near vascularized canals on the bone surface. This was surprising because most PN$^+$ cells were found to be noncycling and FGFR2 was only rarely detected in steady-state periosteum. This suggests that, contrary to more differentiated PN$^+$ cells, FGFR2$^+$ cells are resistant to irradiation. The broader pattern of FGFR2 expression after irradiation also suggests that the population of cells expressing this receptor either expanded or alternatively relocalized to periosteal vascularized canals after irradiation.

To investigate this, we used flow cytometry to quantify the number of both FGFR1- and FGFR2-expressing mesenchymal cells after irradiation (Figure 3B-C). Both Lin$^-$/CD31$^-$/FGFR1$^+$ and Lin$^-$/CD31$^-$/FGFR2$^+$ cell populations were found at a higher frequency in whole bones after TBI, supporting our initial observation that these cells are radio-resistant. However, when we compared their absolute numbers in irradiated bones (n = 10) and nonirradiated controls (n = 5), we observed that their numbers did not significantly increase. One explanation for these observations is that FGFR1/2$^+$ cells do indeed participate in tissue regeneration by giving rise to cells that replace those lost after irradiation; however, these more committed progenies do not express FGFRs. Whereas these results again suggest that FGFR1/2$^+$ mesenchymal cells are radio-resistant and participate in tissue regeneration, it is still unclear whether these cells redistribute in the periosteum from other locations. More detailed studies are needed to assess the kinetics and dynamics of tissue regeneration by FGFR1/2$^+$ cells and their specific contribution to this process.

Isolation of bone-derived FGFR1/2$^+$ MSCs

We next sought to confirm the identity of FGFR1/2$^+$ cells by isolating them for in vitro and in vivo assays. Murine MSCs vary from human MSCs in terms of their ex vivo growth requirements. Indeed, the CFU-F capacity of murine MSCs depends on growth factor supplementation and on their interaction with BM-derived cells.[25] Furthermore, MSCs have a very low frequency in marrow flushes from certain strains of mice.[29,30] Therefore, we isolated FGFR1/2$^+$ mesenchymal cells from whole-bone crushes (including periosteum and perichondrium) and with FGF-2 stimulation. Under these conditions, bone-derived cells proliferated well and showed a dose response to FGF-2 stimulation (Figure 4A). This mitogenic effect was specific to FGF-2 because it could not be recapitulated by any other growth factor tested (EGF, TGF-β, or PDGF) either alone or in combination (Figure 4B). To investigate whether this specific mitogenic effect of FGF-2 could be explained by the absence of other growth factor receptors, we used RT-qPCR to analyze the

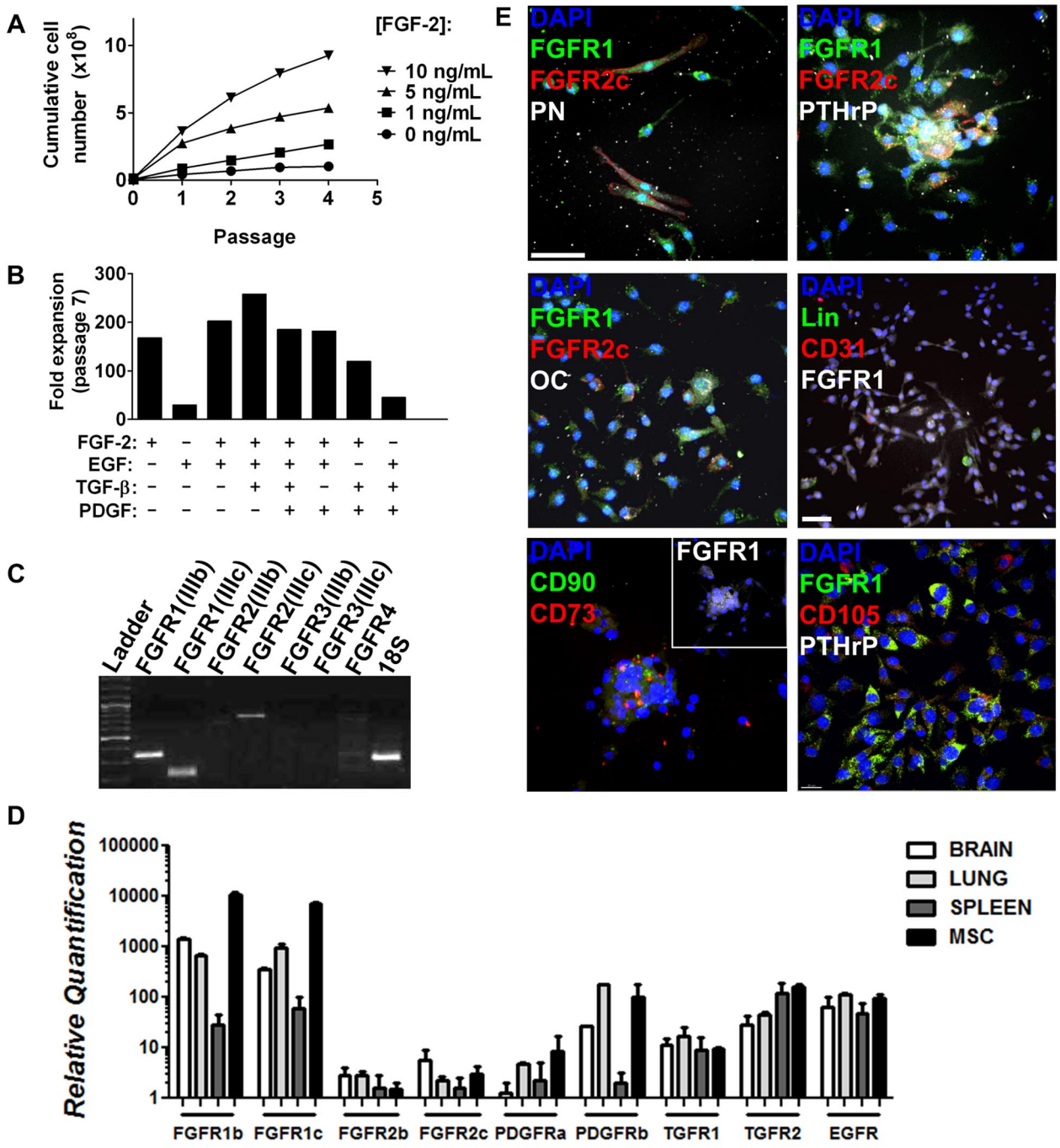

Figure 4. Isolation of FGFR1/2$^+$ skeletal cells in vitro. Plastic adherent skeletal cell preparation from 6- to 8-week-old C57Bl/6 whole-bone digest could be expanded greatly by FGF-2 stimulation in a dose-dependent manner (A). (B) Expansion capacity of whole bone–derived cells in the presence of FGF-2, EGF, TGF-β, and PDGF alone or in combination. Minimal expansion was observed when FGF-2 was absent. Data were calculated from growth curves generated for all conditions using the same initial cell number and harvest conditions. FGFR expression profile of whole bone–derived cells expanded with FGF-2 (98% CD11b$^-$/CD31$^-$/CD45$^-$ by FACS, not shown) at passages 2-5 was analyzed by RT-qPCR, and PCR amplification products were loaded on agarose gel for visualization (passage 5 is shown; C). Liver, brain, and spleen extracts were used as positive controls for the primers (not shown). (D) Relative quantification of the expression of various growth factor receptors expressed by MSCs in vitro as analyzed by RT-qPCR. Cells isolated by whole-bone crush were seeded on coverslips at passage 2 and analyzed by immunofluorescence and confocal microscopy (E). Three-dimensional reconstructions (without deconvolution) of Z-stacks 10-15 μm in depth taken at 0.3-μm intervals are shown. Most cells expressed FGFR1 at various levels, but FGFR2c was limited to rare FGFR1$^+$ cells. FGFR1/2$^+$ cells typically expressed mesenchymal progenitor cell markers such as PN, PTHrP, CD90, CD73, and CD105. Only rare cells expressed osteoblast (osteocalcin, OC), hematopoietic (Lin), or endothelial (CD31) cell markers (see also supplemental Figures 2 and 3). Scale bars indicate 50 μm.

expression of other receptors by MSCs (Figure 4D). We demonstrate that murine MSCs expanded from whole-bone crushes with FGF-2 express high levels of mRNAs encoding PDGFRα, PDGFRβ, TGFβR1, TGFβR2, and EGFR (HER1/ ErbB1). It is therefore likely that MSCs express all of these receptors, which supports what is known about the role of these receptors in bone formation. EGFR is involved in potentiating the effect of FGFR signaling, PGDFRs are known to inhibit MSC differentiation, and TGFβ is mostly known for promoting chondrocytic differentiation.[31,32]

When passaged at low density (5000 cells/cm^2), FACS analysis demonstrated complete absence of hematopoietic, macrophage, and endothelial cell markers as early as passage 2 (Figure 5C). Skeletal

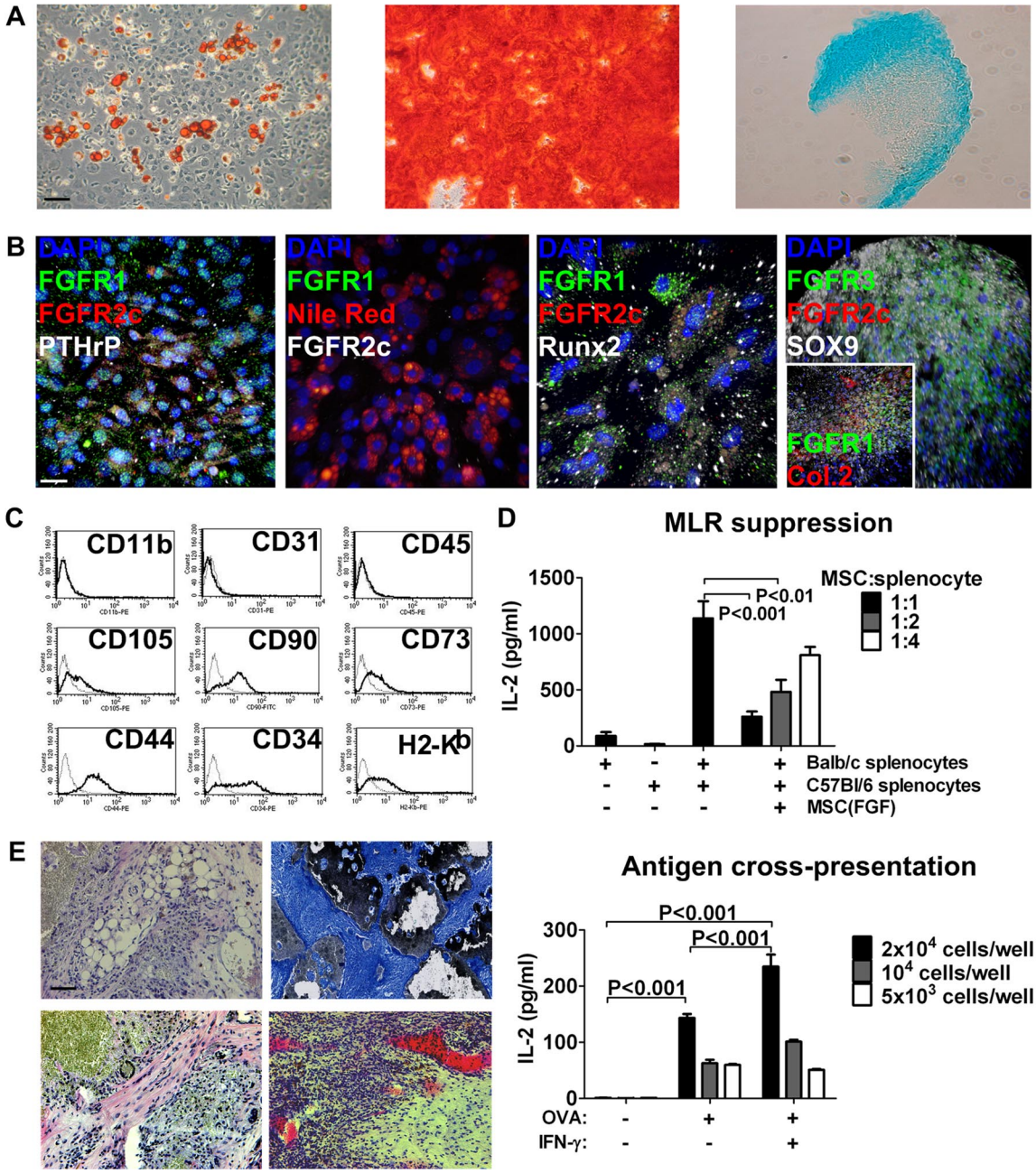

Figure 5. Characterization and MSC phenotype of bone-derived FGFR1/2$^+$ cells in vitro. (A) Left to right: Bone-derived cells expanded with FGF-2 stimulation could produce adipocytes (Oil Red O stain), osteoblasts (Alizarin Red S stain), and chondrocytes (Alcian Blue stain) in vitro and maintained this capacity for at least 10 low-density passages (passage 6 is shown). Scale bar indicates 50 μm. (B) Left to right: Undifferentiated MSCs expanded with FGF-2 expressed FGFR1/2 and PTHrP; MSC-derived Nile Red$^+$ adipocytes lost expression of FGFRs; MSC-derived Runx2$^+$ osteoblasts lost FGFR2 but maintained low FGFR1 expression in some cells; and MSC-derived Sox9$^+$ chondrocytes lost FGFR2 expression but up-regulated FGFR3 (inset shows chondrocyte-specific collagen 2 and expression of FGFR1 in rare undifferentiated cells). Scale bar indicates 25 μm in all panels except the far-right, which indicates 50 μm. (C) FACS analysis of passage-2 MSCs expanded with FGF-2 showing the absence of macrophage (CD11b), endothelial (CD31), and hematopoietic (CD45) cell markers and expression of the C57Bl/6 mesenchymal stem–cell markers CD105, CD90, CD73, CD44, and CD34. These cells also expressed MHC class I (H2-K^b). (D) Top panel: When used as third-party cells in a MLR, FGFR1/2$^+$ MSCs efficiently suppressed T-cell activation (detected as IL-2 production by ELISA) in a dose-dependent manner. Bottom panel: FGFR1/2$^+$ MSCs could process exogenous antigens (in this case, OVA) and cross-present them on MHC I to OVA-responsive T cells. (E) FGFR1/2$^+$ MSCs expanded with FGF-2 for 6 passages were implanted subcutaneously on HA/TCP ceramic particles for 8 weeks. Histological analysis revealed the presence of adipocytes (top left, H&E), osteoblasts (top right, Von Kossa/Toluidine Blue), fibrous tissue (bottom left, H&E), and hematopoietic marrow irrigated by large sinusoids (bottom right, H&E). Scale bar indicates 50 μm.

lineage cells isolated using this technique displayed a typical FGFR isoform expression profile (determined by isoform-specific RT-qPCR) that remained stable throughout serial passaging (Figure 4C passage 5). The cells consistently and exclusively expressed FGFR1(IIIb), FGFR1(IIIc), and FGFR2(IIIc) mRNA, which is consistent with the FGFR expression observed in vivo. Note that we only tested the major isoforms of FGFRs and those that were previously shown to be involved in skeletal development, excluding the soluble isoforms and those lacking the extracellular or kinase domains. Human marrow–derived MSCs from patients $>$ 50 years of age (n = 6) also showed a similar receptor expression profile using RT-qPCR and immunofluorescence (supplemental Figures 2-3 donors shown).

Immunofluorescence staining of passage-2 murine cells revealed that most cells isolated from bone using FGF-2 stimulation

expressed FGFR1 at various levels (Figure 4E). They also coexpressed PN and PTHrP, demonstrating their mesenchymal origin (Figure 4E top panels), and rare FGFR1$^+$/FGFR2$^+$/PN$^+$ cells could also be observed. At passage 2, we observed very few cells expressing osteoblasts (osteocalcin), hematopoietic (Lin), or endothelial (CD31) cell markers (Figure 4E middle panels). However, FGFR1 expression often colocalized with other MSC markers, including CD90, CD73, and CD105 (Figure 4E bottom panels).

We next investigated whether the FGFR1/2$^+$ MSCs we isolated by whole-bone crush originated from the periosteum or marrow (including trabecular bone fraction), the 2 locations where we had identified FGFR1/2$^+$ cells in vivo. FACS analysis revealed that both FGFR1 and FGFR2 were expressed in $< 1\%$ of both periosteum- and BM-derived CD31$^-$/CD45$^-$/Lin$^-$ cells (supplemental Figure 3A). Prospective isolation of these cells using FACS was performed based on the FGFR1 or 2$^+$/Lin$^-$/CD31$^-$/CD41$^-$/CD48$^-$ expression profile to exclude most hematopoietic and endothelial cells. FGFR1/2$^+$ cells proliferated only poorly in vitro when sorted to purity, even in the presence of FGF-2 (not shown) and independently of their origin (periosteum or BM), confirming the observation that murine MSCs require other unidentified factors for expansion.[25] When periosteal/perichondrial cells were cultured with BM cells, small colonies of loosely adherent cells tightly packed together were observed (supplemental Figure 3B). These colonies were highly mobile and attached to a stromal layer, the origin of which is unclear. However, the round colonies were derived from the periosteum because they were never observed in BM flushes. These same colonies were previously found to express MSC markers (Figure 4E). Interestingly, we also observed that most of the CFU-F forming capacity in murine bones was provided by the periosteal fraction of cells, and that bones displaying a higher perichondral surface area (eg, iliac bone vs femur) also displayed increased CFU-F forming capacity (supplemental Figure 3C). These results suggest that MSCs and progenitor cells from different bone compartments are not equivalent, as has also been suggested by other studies.[33-35] It appears that FGFR1/2$^+$ MSCs are more abundant in the periosteum of postnatal mice than in the BM, and that FGF-2 is required but not sufficient for their ex vivo expansion. Direct or paracrine interactions with BM cells are also required, at least at the initial passage, to allow robust expansion of FGFR1/2$^+$ murine MSCs.

Characterization of culture-expanded FGFR1/2$^+$ MSCs

FGFR1/2$^+$ skeletal lineage cells displayed multilineage differentiation capacity in vitro, as judged by their ability to generate adipocytes, osteoblasts, and chondrocytes (Figure 5A passage 5 shown, tested up to passage 10). Interestingly, FGFR1$^+$/FGFR2$^+$/PTHrP$^+$ MSCs completely lost FGFR expression when differentiated into Nile Red$^+$ adipocytes. When differentiated into Runx2$^+$ osteoblasts, only a fraction of cells retained FGFR1 expression and all cells down-regulated FGFR2. After chondrocytic differentiation, Sox9$^+$/collagen2$^+$ chondrocytes robustly up-regulated FGFR3 and only a few undifferentiated cells maintained FGFR1 expression at the periphery of the micromass culture (Figure 5B). Therefore, FGFRs are developmentally regulated in bone-derived FGFR1/2$^+$ MSCs in vitro and their expression recapitulates that of skeletal tissues in vivo.

FGFR1/2$^+$ cells also possessed typical MSC immunosuppressive and immunostimulatory properties (Figure 5D). When used as third-party cells, they could efficiently suppress a MLR in vitro in a dose-dependent manner. Moreover, they could actively process and cross-present exogenous antigens (in this case, OVA) to responsive CD8$^+$ T cells in vitro.

We next investigated the ability of FGFR1/2$^+$ cells to recapitulate bone formation in vivo. Passage-6 cells were implanted subcutaneously on HA/TCP ceramic particles. Implants were retrieved 8 weeks after transplantation and processed for histology. In all retrieved implants ($n = 6$), we observed evidence of bone formation at the periphery of the implants and around ceramic surfaces, as evidenced by positive von Kossa staining (Figure 5E). The pores between ceramic particles contained many adipocytes, dense fibrous tissue, and marrow-like cavities irrigated by large blood vessels, suggesting that culture-expanded FGFR1/2$^+$ MSCs can recapitulate bone formation in vivo.

These results demonstrate that bone-derived FGFR1/2$^+$ of mesenchymal origin display MSC properties when expanded in the presence of FGF-2, including in vitro and in vivo multipotentiality, immunosuppressive and immunostimulatory properties, and expression of cell-surface markers. Our data also demonstrate that undifferentiated murine MSCs express FGFR1b, FGFR1c, and FGFR2c, and that this profile is lost upon cell differentiation or commitment.

Role of FGFRs signaling in MSCs in vitro

The importance of FGF ligands and receptors in bone development, homeostasis, and repair has long been acknowledged.[36,37] However, their exact role has only recently begun to emerge. In MSCs, FGF-2 has been described as a potent mitogen preserving multipotentiality, which we have confirmed here in FGFR1/2$^+$ murine MSCs. Conversely, murine MSCs expanded without FGF-2 stimulation displayed distinct characteristics of cellular senescence very early after the initial isolation. We observed increased senescence-associated β-Gal activity, morphological changes (increased cell diameter and disruption of the actin cytoskeleton), and growth arrest (decreased proliferation and Ki67 expression) in early-passage MSCs expanded without FGF-2 compared with FGF-2–stimulated MSCs (Figure 6A and supplemental Figure 4A). In FGF-2–stimulated passage-3 MSCs, 54.7% of the cells were found to be Ki67$^+$ (123 Ki67$^+$ cells of 225 total cells counted), whereas without FGF-2, only 11.3% (8 of 80) expressed Ki67. These results suggest that in addition to its mitogenic effects, FGF-2 signaling through FGFR1/2 may be involved in regulating senescence in MSCs in vitro.

Murine cells, and in particular MSCs, are known to undergo rapid immortalization in vitro. We therefore tested whether the mitogenic effect of FGF-2 on MSCs was in fact an immortalizing effect. To do this, we isolated MSCs and expanded them in the presence of FGF-2 for 3 low-density passages, at which point FGF-2 was removed from the growth medium (Figure 6B). We observed that removal of the growth factor immediately induced growth arrest in MSCs, which was evidenced by decreased proliferation and down-regulation of the proliferation marker Ki67 from 46.4% (247 of 532) to 17.9% (29 of 162). We also observed that the senescent phenotype of MSCs expanded without FGF-2 could not be rescued by the subsequent addition of the growth factor. To further confirm that FGF-2–stimulated MSCs were not immortalized, we investigated whether they were still able to undergo cellular senescence. We expanded MSCs on coverslips with or without FGF-2 and irradiated them at 10 Gy. Seven days later, we analyzed the cells for evidence of a senescent phenotype. We observed that MSCs expanded with FGF-2 were still capable of undergoing senescence (increased senescence-associated β-Gal activity, morphological changes, and growth arrest; Figure 6C).

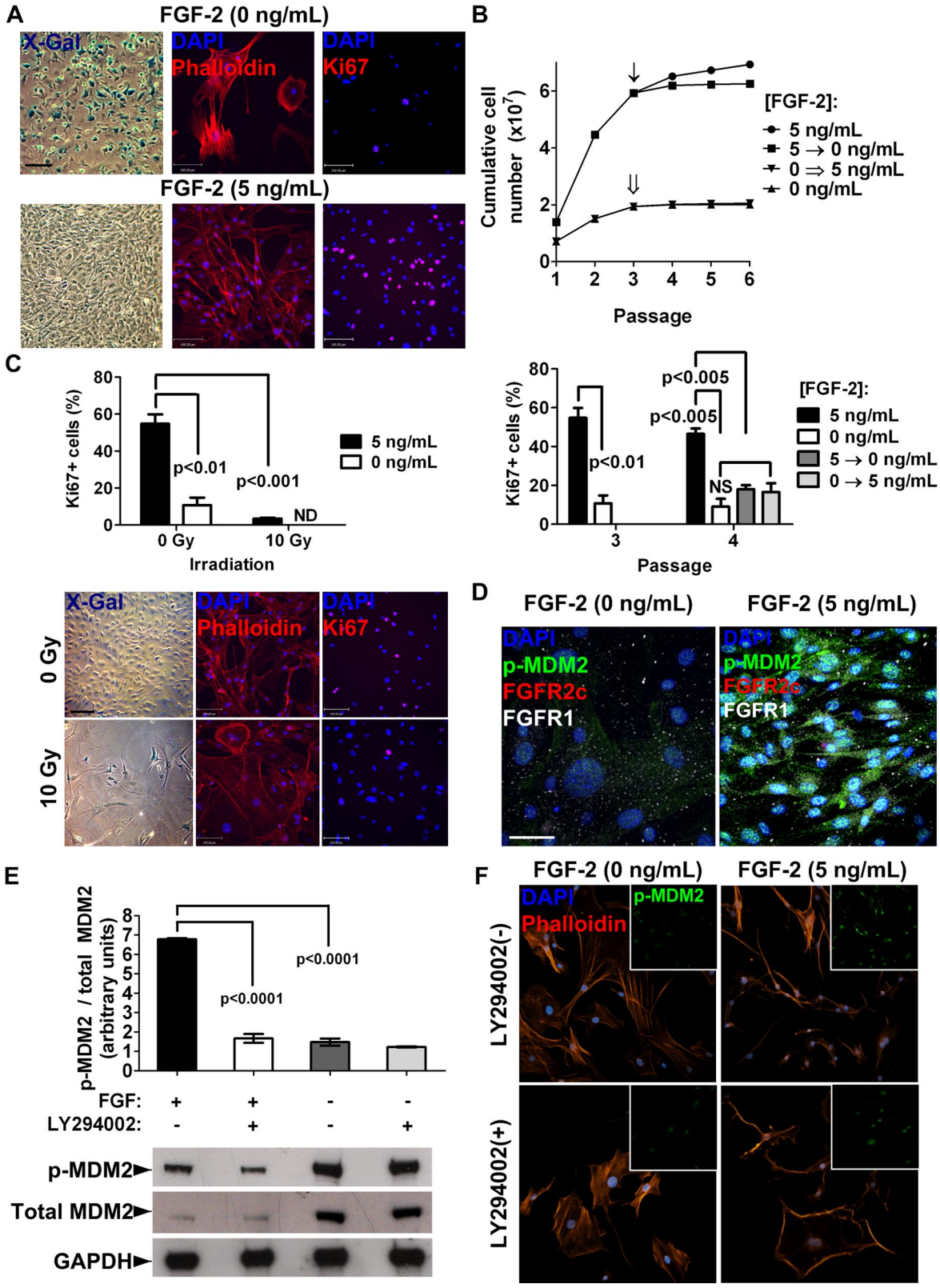

Figure 6. Inhibition of cellular senescence by FGF-2 in MSCs in vitro. (A) FGFR1/2$^+$ MSCs displayed a characteristic senescent phenotype as early as passage 2 when expanded without FGF-2, including up-regulation of senescence-associated β-Gal (X-Gal staining), increased cell diameter (see also supplemental Figure 4A), morphological changes, disruption of the actin cytoskeleton (phalloidin staining), and growth arrest (decreased Ki67 staining). Scale bars indicate 50 μm for X-Gal and 100 μm for phalloidin and Ki67. (B) Growth curves and Ki67 expression of MSCs culture expanded with or without FGF-2 stimulation for 3 passages, at which point the culture conditions were switched (arrow and double arrow). See "Results" for the numbers of cells counted. (C) Induction of cellular senescence in FGF-2–stimulated MSCs at passage 3 by irradiation at 10 Gy shown by growth arrest (lower Ki67; top panel) and adoption of a senescent phenotype (bottom panel) indicate that MSCs were not immortalized. Scale bars indicate 50 μm for X-Gal and 100μm for phalloidin and Ki67. ND indicates not detected. (D) FGFR1/2$^+$ MSCs lost expression of FGFRs when induced into senescence, as shown by decreased p-MDM2(Ser186) by FGF-2 starvation for 48 hours. Scale bar indicates 25 μm. (E) Western blot and densitometry showing that FGF-2 stimulation of FGFR1/2$^+$ MSCs resulted in hyperphosphorylation of MDM-2 on Ser186, which could be inhibited by the PI3K/AKT inhibitor LY294002. This experiment was performed in triplicate. (F) Immunofluorescence and confocal analysis confirmed that FGF-2 stimulation of FGFR1/2$^+$ MSCs resulted in hyperphosphorylation and increased nuclear localization of MDM2 in a PI3K/AKT–dependent manner (see also supplemental Figure 4C). Scale bar indicates 50 μm.

After irradiation, the percentage of Ki67$^+$ cells sharply decreased from 54.7% (123 of 225) to 3.5% (10 of 287). These results indicate that FGF-2 stimulation inhibits cellular senescence in MSCs in vitro without immortalization, whereas the lack of FGF-2 stimulation induces irreversible senescence of MSCs.

To understand the mechanism by which FGF-2 inhibited cellular senescence in MSCs, we assayed intracellular regulators of senescence in mice (eg, p19/ARF and MDM2) in freshly isolated MSCs in vitro (we used negative selection to enrich for mesenchymal cells and to minimize interference from hematopoietic cells). p19/ARF levels were found to be quickly up-regulated (passage 0) in MSCs grown with or without FGF-2 (supplemental Figure 4B), and therefore are unlikely to be involved in FGF-2–mediated inhibition of cellular senescence. However, we observed a significant hyperphosphorylation of MDM2 on Ser186 in FGF-2–stimulated MSCs, and also observed that hypophosphorylation of MDM2 in nontreated cells correlated well with loss of FGFR1 expression in senescent cells (Figure 6D).

Because Ser186 on MDM2 is a direct target of AKT, which is also known to be downstream of FGFR signaling, we also investigated whether the PI3K/AKT inhibitor LY294002 could suppress FGF-2–mediated hyperphosphorylation of MDM2 and the ensuing inhibition of cellular senescence. We found that although cells grown without FGF-2 express more total MDM2 protein, it is hypophosphorylated relative to FGF-2–treated cells (Figure 6E). Inhibition of the PI3K/AKT pathway during FGF-2 stimulation also decreased relative phospho-MDM2/total MDM2 levels. Immunofluorescence staining confirmed these observations (Figure 6F), and showed that both the absence of FGF-2 and inhibition of the PI3K/AKT pathway decreased p-MDM2 levels and nuclear translocation (supplemental Figure 4C) and profoundly affected cell morphology. It is well established that phosphorylation of MDM2 on Ser186 and subsequent nuclear translocation promotes its ubiquitin ligase activity toward p53, targeting the latter for degradation by the proteasome.[38-40] This could account for the inhibition of cellular senescence observed in FGF-2–treated MSCs in vitro.

Our results demonstrate that FGF-2 efficiently inhibits cellular senescence in FGFR1/2$^+$ MSCs in vitro by promoting hyperphosphorylation of MDM2 on Ser186 and its nuclear localization in a PI3K/AKT-dependent manner. Moreover, our data suggest that this effect is reversible and that FGF-2 promotes expansion of murine MSCs without immortalization.

Discussion

At the earliest stage of endochondral bone formation, FGFR2c$^+$ mesenchymal cells aggregate and condense in response to signals from the apical ectodermal ridge. Cells at the center of the aggregation then differentiate into chondrocytes and lose FGFR2 before up-regulating FGFR3, whereas cells at the periphery of the aggregation form a perichondrium layer of undifferentiated mesenchymal cells expressing FGFR1/2.[17,20] During postnatal life, FGFR1 is detected in the periosteum and in trabecular bone–lining cells in mice, but little is known about the identity of these cells.[41] Indeed, FGFR ligand systems are difficult to study using genetic methods because of their broad tissue distribution, promiscuous ligand usage by receptors, redundancy in specificity and effects of various ligands, alternate exon usage after isoform-specific deletions of receptors, and the fact that complete knockout of FGFR1 or FGFR2 causes early embryonic lethality. However, the role of perichondrium-derived FGF-18 signaling through FGFR3 expressed in chondrocytes has been well documented in the regulation of growth plate cartilage.[42,43]

Vascular invasion induces osteogenic commitment of perichondrial cells. These cells migrate along blood vessels (as pericytes) to create the bone collar (cortical bone). Blood vessels entering the bone cavities and lacunae left by hypertrophic chondrocyte apoptosis also carry these MSC-like cells to create the primary spongiosa, marrow space, and eventually the secondary ossification center. This model of endochondral bone formation was recently confirmed by 2 different studies demonstrating that the perichondrium gives rise to cells that participate in both cortical and trabecular bone formation.[4,5,33] However, it appears that perivascular cells are downstream of more primitive perichondrial MSCs that would give rise to growth plate chondrocytes, cortical bone osteoblasts/osteocytes, and the osteostromal progenitors (pericytes) that colonize the primary spongiosa (possibly the collagen 2–expressing chondro-perichondrial progenitor proposed by Maes et al[5]). This primitive MSC remains elusive, and its exact niche, fate, and potential in postnatal bones remain obscure.

The data presented here provide new tools with which to examine these questions in more detail in future studies. We provide evidence that primitive MSCs are enriched in the FGFR1/2$^+$ fraction of perichondrial/periosteal cells in murine bones. These cells are also present in postnatal bones, where they express early mesenchymal cell markers. Furthermore, perichondrial FGFR1/2$^+$ cells appear to play a role in normal tissue homeostasis (or growth) because they express the proliferation marker Ki67 at steady state. The fact that the FGFR1/2$^+$ cells are radio-resistant and redistribute to new niches after TBI also suggests that these cells participate in tissue repair, although more studies are needed to confirm these observations.

The FGFR1/2$^+$ MSCs identified in murine bones could be isolated and culture expanded when stimulated with FGF-2. These cells displayed all properties typically associated with MSCs, including multipotentiality (in vitro and in vivo), expression of cell-surface markers, and immunomodulatory properties. Moreover, their expression of FGFRs was modulated during differentiation into skeletal lineage cells, recapitulating the FGFR-expression profile in native bone tissues. Therefore, we suggest that FGFR expression can be used to identify primitive MSCs in embryonic and postnatal bones from their more differentiated progeny (Figure 7). This might prove useful in the following ways: (1) to study MSCs and their progeny in their native bone/marrow niches and in vitro; (2) to devise standard isolation and expansion methods for high-quality MSCs; (3) to study MSCs in animal models such as mice; and (4) to help cell therapists and tissue engineers better understand the potential and requirements of MSCs. However, more precise lineage-tracing studies will be required to fully validate the model we propose, in particular to elucidate the exact lineage relationship between FGFR2$^+$ and FGFR1$^+$ cells. Another outstanding question that remains to be solved relates to the fate of FGFR2$^+$ cells after growth plate closure, and whether these cells disappear from mature bones or relocalize to other, as-yet-unidentified niches.

Nevertheless, our data provide key insights into the role of FGF signaling in MSCs. We found that FGF-2 stimulated activation of the PI3K/AKT pathway, leading to hyperphosphorylation of MDM2 on Ser186 and nuclear translocation. It appears that FGF-2, in addition to its well-known mitogenic effects, protects MSCs from proliferation-induced cellular senescence and immortalization and could therefore play a key role in self-renewal and maintenance of

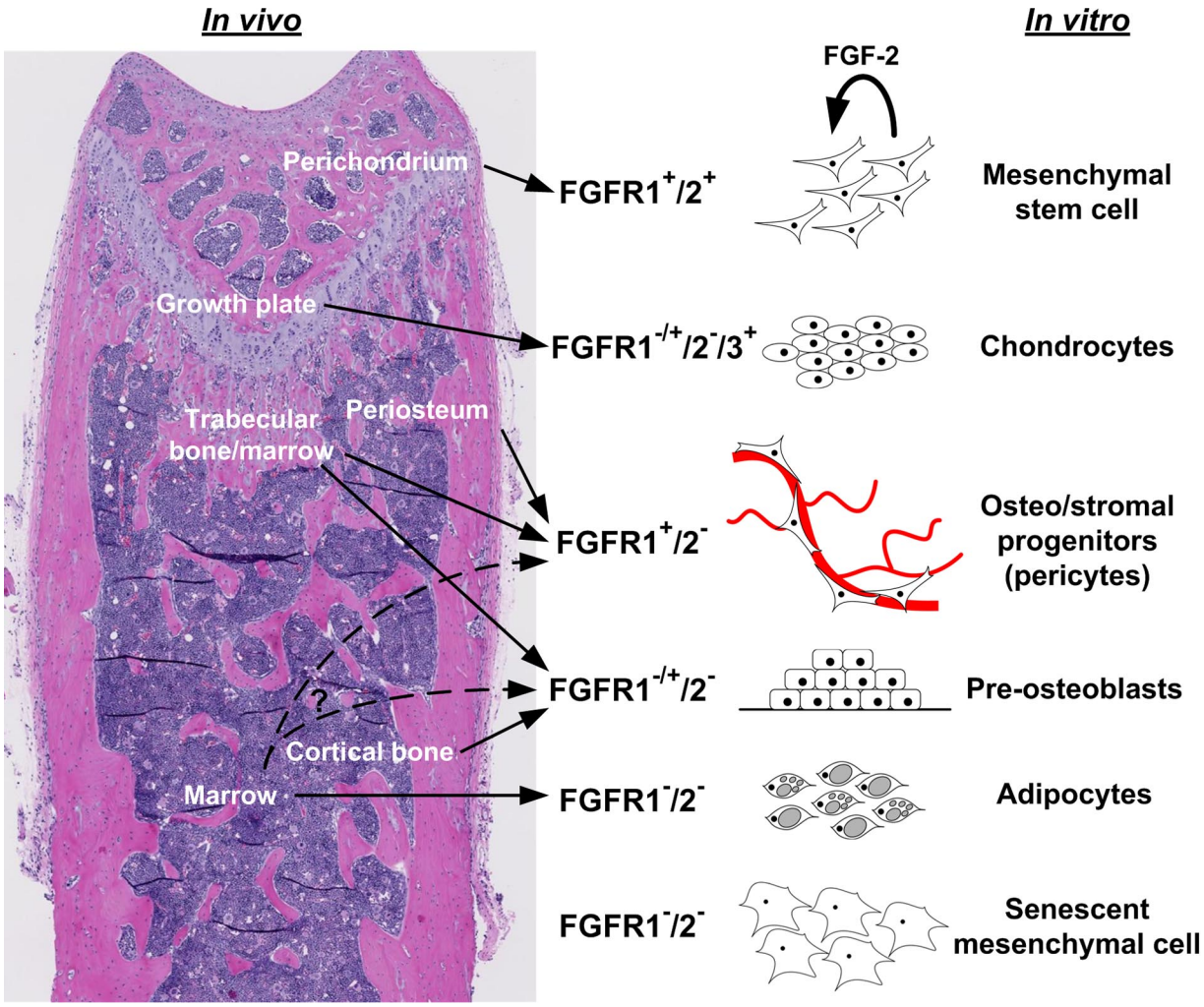

Figure 7. Model of developmental regulation of FGFRs in MSCs and skeletal tissues. Simplified working model based on findings presented here and in other studies.[4,5,33] Undifferentiated mesenchymal cells expressed FGFR1/2 in the perichondrium and in vitro and appeared to self-renew in vitro upon FGF-2 signaling (proliferation with maintenance of MSC properties). Upon chondrogenic differentiation in the growth plate or in vitro, mesenchymal cells lost FGFR1/2 expression but up-regulated FGFR3. However, FGFR1 was expressed in hypertrophic chondrocytes. More committed mesenchymal progenitors in cortical and trabecular perivascular space and in vitro expressed FGFR1 to various degrees, but rarely expressed FGFR2. MSC-derived differentiated osteoblasts and stromal elements (eg, adipocytes) did not express FGFRs.

stemness in MSCs. It will be interesting to determine whether FGF signaling in MSCs plays the same role in vivo.

In summary, we have found that MSCs derived from postnatal murine and human bones express both FGFR1 and FGFR2. These markers can be used to identify early mesenchymal progenitors in vivo and in vitro. FGFR1/2$^+$ skeletal cells display and maintain a characteristic MSC phenotype when expanded in the presence of FGF-2 for up to 12 passages. The effect of FGF-2 on MSC senescence suggests a role in licensing the self-renewing proliferation of MSCs in vitro.

Acknowledgments

We thank Dr Ian Copland (Emory University), Dr Christian Beauséjour (Centre Hospitalier Universitaire Ste-Justine, Université de Montréal), and Dr Janet Henderson (McGill University) for useful discussions and comments on the manuscript; Christian Young and the Montreal Center for Experimental Therapy of Cancer Flow Cytometry and Imaging Facility for assistance with cytometry and confocal microscopy; and Cory Glowinski (Bitplane, Zurich, Switzerland) and Dr Andrew Mouland (McGill University) for assistance with the Imaris software.

This study was funded by the Fonds de la recherche en santé du Québec and by the Canadian Institutes of Health Research.

Authorship

Contribution: D.L.C. and M.F. designed the study, performed all experiments, analyzed the data, and wrote the manuscript; and J.G. supervised the project, analyzed the data, and revised the manuscript.

Conflict-of-interest disclosure: The authors declare no competing financial interests.

Correspondence: Dr Jacques Galipeau, MD, FRCP(C), Professor of Hematology and Medical Oncology, Pediatrics & Medicine, Emory University, 1365 Clifton Rd, Clinic B, Suite 5100-5117, Atlanta, GA 30322; e-mail: jgalipe@emory.edu.

References

1. Bianco P, Robey PG, Simmons PJ. Mesenchymal stem cells: revisiting history, concepts, and assays. *Cell Stem Cell*. 2008;2(4):313-319.
2. Phinney DG. Building a consensus regarding the nature and origin of mesenchymal stem cells. *J Cell Biochem Suppl*. 2002;38:7-12.
3. Bianco P, Robey PG, Saggio I, Riminucci M. "Mesenchymal" stem cells in human bone marrow (skeletal stem cells): a critical discussion of their nature, identity, and significance in incurable skeletal disease. *Hum Gene Ther*. 2010;21(9): 1057-1066.
4. Colnot C, Lu C, Hu D, Helms JA. Distinguishing the contributions of the perichondrium, cartilage, and vascular endothelium to skeletal development. *Dev Biol*. 2004;269(1):55-69.
5. Maes C, Kobayashi T, Selig MK, et al. Osteoblast precursors, but not mature osteoblasts, move into developing and fractured bones along with invading blood vessels. *Dev Cell*. 2010;19(2):329-344.
6. Kronenberg HM. The role of the perichondrium in fetal bone development. *Ann N Y Acad Sci*. 2007; 1116:59-64.
7. Maes C, Kobayashi T, Kronenberg HM. A novel transgenic mouse model to study the osteoblast lineage in vivo. *Ann N Y Acad Sci*. 2007;1116: 149-164.
8. Sacchetti B, Funari A, Michienzi S, et al. Self-renewing osteoprogenitors in bone marrow sinusoids can organize a hematopoietic microenvironment. *Cell*. 2007;131(2):324-336.
9. Crisan M, Yap S, Casteilla L, et al. A perivascular origin for mesenchymal stem cells in multiple human organs. *Cell Stem Cell*. 2008;3(3):301-313.
10. Short BJ, Brouard N, Simmons PJ. Prospective isolation of mesenchymal stem cells from mouse compact bone. *Methods Mol Biol*. 2009;482:259-268.
11. De Bari C, Dell'accio F, Vanlauwe J, et al. Mesenchymal multipotency of adult human periosteal cells demonstrated by single-cell lineage analysis. *Arthritis Rheum*. 2006;54(4):1209-1221.
12. Tuli R, Tuli S, Nandi S, et al. Characterization of multipotential mesenchymal progenitor cells derived from human trabecular bone. *Stem Cells*. 2003;21(6):681-693.
13. Allen MR, Hock JM, Burr DB. Periosteum: biology, regulation, and response to osteoporosis therapies. *Bone*. 2004;35(5):1003-1012.
14. Diaz-Flores L, Gutierrez R, Lopez-Alonso A, Gonzalez R, Varela H. Pericytes as a supplementary source of osteoblasts in periosteal osteogenesis. *Clin Orthop Relat Res*. 1992;275:280-286.
15. Reilly TM, Seldes R, Luchetti W, Brighton CT. Similarities in the phenotypic expression of pericytes and bone cells. *Clin Orthop Relat Res*. 1998;346:95-103.
16. Brighton CT, Lorich DG, Kupcha R, Reilly TM, Jones AR, Woodbury RA. The pericyte as a possible osteoblast progenitor cell. *Clin Orthop Relat Res*. 1992;275:287-299.
17. Kronenberg HM. Developmental regulation of the growth plate. *Nature*. 2003;423(6937):332-336.
18. Karsenty G. The complexities of skeletal biology. *Nature*. 2003;423(6937):316-318.
19. Mariani FV, Martin GR. Deciphering skeletal patterning: clues from the limb. *Nature*. 2003; 423(6937):319-325.
20. Ornitz DM, Marie PJ. FGF signaling pathways in endochondral and intramembranous bone development and human genetic disease. *Genes Dev*. 2002;16(12):1446-1465.
21. Baddoo M, Hill K, Wilkinson R, et al. Characterization of mesenchymal stem cells isolated from murine bone marrow by negative selection. *J Cell Biochem*. 2003;89(6):1235-1249.
22. Solchaga LA, Penick K, Goldberg VM, Caplan AI, Welter JF. Fibroblast growth factor-2 enhances proliferation and delays loss of chondrogenic potential in human adult bone-marrow-derived mesenchymal stem cells. *Tissue Eng Part A*. 2010; 16(3):1009-1019.
23. Bianchi G, Banfi A, Mastrogiacomo M, et al. Ex vivo enrichment of mesenchymal cell progenitors by fibroblast growth factor 2. *Exp Cell Res*. 2003; 287(1):98-105.
24. Tsutsumi S, Shimazu A, Miyazaki K, et al. Retention of multilineage differentiation potential of mesenchymal cells during proliferation in response to FGF. *Biochem Biophys Res Commun*. 2001;288(2):413-419.
25. Kuznetsov SA, Friedenstein AJ, Robey PG. Factors required for bone marrow stromal fibroblast colony formation in vitro. *Br J Haematol*. 1997; 97(3):561-570.
26. Kiel MJ, Yilmaz OH, Iwashita T, Yilmaz OH, Terhorst C, Morrison SJ. SLAM family receptors distinguish hematopoietic stem and progenitor cells and reveal endothelial niches for stem cells. *Cell*. 2005;121(7):1109-1121.
27. Blumer MJ, Schwarzer C, Perez MT, Konakci KZ, Fritsch H. Identification and location of bone-forming cells within cartilage canals on their course into the secondary ossification centre. *J Anat*. 2006; 208(6):695-707.
28. Fukushi J, Inatani M, Yamaguchi Y, Stallcup WB. Expression of NG2 proteoglycan during endochondral and intramembranous ossification. *Dev Dyn*. 2003;228(1):143-148.
29. Phinney DG, Kopen G, Isaacson RL, Prockop DJ. Plastic adherent stromal cells from the bone marrow of commonly used strains of inbred mice: variations in yield, growth, and differentiation. *J Cell Biochem*. 1999;72(4):570-585.
30. Peister A, Mellad JA, Larson BL, Hall BM, Gibson LF, Prockop DJ. Adult stem cells from bone marrow (MSCs) isolated from different strains of inbred mice vary in surface epitopes, rates of proliferation, and differentiation potential. *Blood*. 2004;103(5):1662-1668.
31. Miraoui H, Marie PJ. Fibroblast growth factor receptor signaling crosstalk in skeletogenesis. *Sci Signal*. 2010;3(146):re9.
32. Augello A, De Bari C. The regulation of differentiation in mesenchymal stem cells. *Hum Gene Ther*. 2010;21(10):1226-1238.
33. Colnot C. Skeletal cell fate decisions within periosteum and bone marrow during bone regeneration. *J Bone Miner Res*. 2009;24(2):274-282.
34. Yoshimura H, Muneta T, Nimura A, Yokoyama A, Koga H, Sekiya I. Comparison of rat mesenchymal stem cells derived from bone marrow, synovium, periosteum, adipose tissue, and muscle. *Cell Tissue Res*. 2007;327(3):449-462.
35. Arai F, Ohneda O, Miyamoto T, Zhang XQ, Suda T. Mesenchymal stem cells in perichondrium express activated leukocyte cell adhesion molecule and participate in bone marrow formation. *J Exp Med*. 2002;195(12):1549-1563.
36. Chen L, Deng CX. Roles of FGF signaling in skeletal development and human genetic diseases. *Front Biosci*. 2005;10:1961-1976.
37. Naski MC, Ornitz DM. FGF signaling in skeletal development. *Front Biosci*. 1998;3:d781-d794.
38. Meek DW, Hupp TR. The regulation of MDM2 by multisite phosphorylation–opportunities for molecular-based intervention to target tumours? *Semin Cancer Biol*. 2010;20(1):19-28.
39. Meek DW, Knippschild U. Posttranslational modification of MDM2. *Mol Cancer Res*. 2003;1(14): 1017-1026.
40. Lu X. Tied up in loops: positive and negative autoregulation of p53. *Cold Spring Harb Perspect Biol*. 2010;2(5):a000984.
41. Jacob AL, Smith C, Partanen J, Ornitz DM. Fibroblast growth factor receptor 1 signaling in the osteo-chondrogenic cell lineage regulates sequential steps of osteoblast maturation. *Dev Biol*. 2006;296(2):315-328.
42. Liu Z, Lavine KJ, Hung IH, Ornitz DM. FGF18 is required for early chondrocyte proliferation, hypertrophy and vascular invasion of the growth plate. *Dev Biol*. 2007;302(1):80-91.
43. Davidson D, Blanc A, Filion D, et al. Fibroblast growth factor (FGF) 18 signals through FGF receptor 3 to promote chondrogenesis. *J Biol Chem*. 2005;280(21):20509-20515.